On the modeling of elastic solids by using orthonormal dual tensors

T. Merlini M. Morandini

merlini@aero.polimi.it morandini@aero.polimi.it

Abstract

A new modeling of elastic solids capable of polar description is presented. The primary d.o.f. of a material particle is the rototranslation as a whole. By resorting to the algebra of dual numbers, the rototranslation is represented by an orthonormal dual tensor that inherits all the properties of the rotation. A variational formulation fit for the proposed modeling is outlined and reduced to the case of non-polar materials. The discrete problem exploits consistent multiplicative interpolation and updating technique of the kinematical field. The first results of the finite-element implementation concern simulations of high geometrical nonlinearities in bending dominated problems.

1 Introduction

Formulations in solid mechanics based on the rotation as an independent field, for the analysis of either couple-stress carrying materials or common non-polar materials, are reaching a high maturity level [6, 20, 18, 2, 10, 17, 19, 5]. Polar descriptions go back to the Cosserat's; however, it is only in the recent past, thanks to the growing familiarity with finite rotations (e.g. [3]), that finite elements endowed with rotational dof's have been developed for geometrically nonlinear problems in elasticity, e.g. [9, 11]. Progress in this field is often furthered by advances in shell theories and elements and beam formulations (an extensive literature covers this subject).

However, the *modeling* of the continuum keeps on being always the classical one. The orientation of the material particles is a distinct field superposed to the underlying field of the position. As a matter of fact, the two kinematical quantities that fully locate a material particle are intrinsically and deeply different in character: the position belongs to the Euclidean vector space, while the orientation is an element of a special orthogonal group. In the classical modeling, the Euclidean position field is privileged and is made fully responsible of the metric, hence of the configuration of the continuum. This approach may prove subtle when differentiating and interpolating the kinematical fields — a standard process in finite-element approximations of variational principles. For instance, the interpolation over a finite domain will produce first an interpolated position, and just there an interpolated orientation.

An alternative modeling is proposed which brings the quantity identifying the position into a richer quantity encompassing both position and orientation, and endowed with the geometric and differential properties of a wider special orthogonal

manifold. This modeling and its computational implementation are described at length in a paper about to appear in literature [16].

2 Oriento-position and rototranslation

Let's consider a frame of independent vectors $\boldsymbol{\alpha}_j$ $(j = 1, 2, 3)$ detaching from a point in the 3D space. For simplicity, refer to an orthonormal triad, made of orthogonal unit vectors. Also consider another similar frame $\boldsymbol{\alpha}'_j$ applied at another point. Once an origin and an orthonormal triad $\boldsymbol{i}_j$ are chosen as a reference frame, the two frames become identified by the position vectors $\boldsymbol{x} = x_j\, \boldsymbol{i}^j$ and $\boldsymbol{x}' = x'_j\, \boldsymbol{i}^j$ and the orientation tensors $\boldsymbol{\alpha} = \boldsymbol{\alpha}_j \otimes \boldsymbol{i}^j$ and $\boldsymbol{\alpha}' = \boldsymbol{\alpha}'_j \otimes \boldsymbol{i}^j$, respectively. Positions are measured by the distances from the origin, while orientations are measured by the relative rotations from the identity tensor $\boldsymbol{I} = \boldsymbol{i}_j \otimes \boldsymbol{i}^j$. The position $\boldsymbol{x}'$ is the position $\boldsymbol{x}$ plus the 'displacement' $\boldsymbol{u} = \boldsymbol{x}' - \boldsymbol{x}$, instead the orientation $\boldsymbol{\alpha}'$ is the orientation $\boldsymbol{\alpha}$ rotated by tensor $\boldsymbol{\Phi} = \boldsymbol{\alpha}'\boldsymbol{\alpha}^{\mathrm{T}}$. Clearly, positions belong to the Euclidean vector space, while orientations are elements of the special orthogonal manifold.

Then, introduce the dual tensor

$$\begin{aligned} \boldsymbol{A} &= \boldsymbol{X}\, \boldsymbol{\alpha} \\ &= (\boldsymbol{I} + \epsilon\, \boldsymbol{x}\times)\, \boldsymbol{\alpha}\,, \end{aligned} \tag{1}$$

where $\times$ is the usual symbol for the cross-product operator, and $\boldsymbol{x}\times$ denotes the skew-symmetric tensor with $\boldsymbol{x}$ as axial vector. A dual tensor embodies two distinct tensors, referred to as the primal part and the dual part [1]. The explicit expression of a dual tensor is the sum of the primal part and the dual part multiplied by the dual unity ϵ — a number endowed with the properties $\epsilon \neq 0$ and $\epsilon^2 = \epsilon^3 = \cdots = 0$. We recognize in the primal part of dual tensor $\boldsymbol{\alpha} + \epsilon\, \boldsymbol{x} \times \boldsymbol{\alpha}$ in Eq. (1) the orientation tensor itself, while the dual part is the 'moment' tensor of the orientation with respect to the origin as a *pole*. The algebra of dual numbers ensures that $\boldsymbol{A}^{-1} = \boldsymbol{A}^{\mathrm{T}}$, hence dual tensor $\boldsymbol{A}$ is orthonormal. The pole-based dual tensor $\boldsymbol{A}$ is referred to as the *oriento-position* tensor, since it is able to represent both position and orientation of an applied frame within a single orthonormal entity. It allows the multiplicative decomposition into an orientation tensor $\boldsymbol{\alpha}$ and a position tensor $\boldsymbol{X}$, which is by itself a pole-based orthonormal dual tensor.

Oriento-positions are elements of a special orthogonal manifold of dual tensors, referred to as *rototranslation* tensors. Rototranslations are magnitude-preserving transformations of pole-based geometrical objects like the pair vector and moment, which are conveniently represented by dual vectors and tensors. A rototranslation tensor is a pole-based dual tensor that must comply with the form

$$\begin{aligned} \boldsymbol{H} &= \boldsymbol{T}\, \boldsymbol{\Phi} \\ &= (\boldsymbol{I} + \epsilon\, \boldsymbol{t}\times)\, \boldsymbol{\Phi}\,, \end{aligned}$$

having a rotation tensor $\boldsymbol{\Phi}$ as primal part and a dual part like $\boldsymbol{t} \times \boldsymbol{\Phi}$; vector $\boldsymbol{t}$ is called the translation vector and the orthonormal dual tensor $\boldsymbol{T}$ the translation tensor. Oriento-positions in space are measured by the relative rototranslations from the identity tensor placed at the origin. So, the second applied frame is identified by a different dual tensor $\boldsymbol{A}'$, based on the same pole, that corresponds to the oriento-position $\boldsymbol{A}$ rototranslated by tensor $\boldsymbol{H} = \boldsymbol{A}'\boldsymbol{A}^{\mathrm{T}} = \boldsymbol{X}'\boldsymbol{\Phi}\boldsymbol{X}^{\mathrm{T}}$, made of a rotation $\boldsymbol{\Phi}$

$= \boldsymbol{\alpha}'\boldsymbol{\alpha}^{\mathrm{T}}$ and a translation $\boldsymbol{t} = \boldsymbol{x}' - \boldsymbol{\Phi}\boldsymbol{x}$ (a vector far different from the displacement $\boldsymbol{u} = \boldsymbol{x}' - \boldsymbol{x}$).

Rototranslations inherit all the properties of rotations. They compose multiplicatively and do not commute. Moreover, they are endowed with an exponential map and its inverse logarithmic map, $\boldsymbol{H} = \exp(\boldsymbol{\eta}\times)$ and $\boldsymbol{\eta}\times = \log(\boldsymbol{H})$, which introduce the *helix* $\boldsymbol{\eta} = \boldsymbol{\varphi} + \epsilon\,\boldsymbol{\rho}$ as the appropriate dual vector for the natural parameterization of rototranslations. Differentiation of the orthonormality condition $\boldsymbol{H}^{\mathrm{T}}\boldsymbol{H} = \boldsymbol{I}$ leads to the differential helices characterizing the subsequent variations of a rototranslation tensor. By taking independent variations d, ∂ and δ, the lowest three characteristic differential helices are conveniently defined as the axials of the following tensors [12],

$$\begin{aligned} d\boldsymbol{H}\boldsymbol{H}^{\mathrm{T}} &= \boldsymbol{\eta}_d\times \\ d\partial\boldsymbol{H}\boldsymbol{H}^{\mathrm{T}} &= \boldsymbol{\eta}_{d\partial}\times + \tfrac{1}{2}\,(\boldsymbol{\eta}_d\times\boldsymbol{\eta}_\partial\times + \boldsymbol{\eta}_\partial\times\boldsymbol{\eta}_d\times) \\ d\partial\delta\boldsymbol{H}\boldsymbol{H}^{\mathrm{T}} &= \boldsymbol{\eta}_{d\partial\delta}\times + \tfrac{1}{2}\,(\boldsymbol{\eta}_{d\partial}\times\boldsymbol{\eta}_\delta\times + \boldsymbol{\eta}_{\partial\delta}\times\boldsymbol{\eta}_d\times + \boldsymbol{\eta}_{\delta d}\times\boldsymbol{\eta}_\partial\times \\ &\qquad + \boldsymbol{\eta}_d\times\boldsymbol{\eta}_{\partial\delta}\times + \boldsymbol{\eta}_\partial\times\boldsymbol{\eta}_{\delta d}\times + \boldsymbol{\eta}_\delta\times\boldsymbol{\eta}_{d\partial}\times)\,, \end{aligned} \tag{2}$$

the symmetric part being dependent on lower-order differential helices. Appropriate differential maps relate the characteristic dual vectors to the variations of the helix itself [14]. In particular, the first differential map $\boldsymbol{\eta}_d = \boldsymbol{\Lambda}\,d\boldsymbol{\eta} = \boldsymbol{\Lambda}\,\mathrm{ax}\,d\log(\boldsymbol{H})$ governs the tangent space of the rototranslation. The differential maps are also of interest in the explicit representation of rototranslations; the first differential map of rotation $\boldsymbol{\varphi}_d = \boldsymbol{\Gamma}\,d\boldsymbol{\varphi}$, for instance, is the same map relating the translation vector to the linear part of the helix, $\boldsymbol{t} = \boldsymbol{\Gamma}\boldsymbol{\rho}$.

3 The helicoidal modeling

In the light of a polar description, the configuration of a deformable continuum is determined by the position and orientation of each material particle. The pole-based oriento-position tensor $\boldsymbol{A}$ is an alternative choice of configuration variables to the classical pair, position vector $\boldsymbol{x}$ and orientation tensor $\boldsymbol{\alpha}$. However, the nonlinear change of variables Eq. (1) entails remarkable differences as far as concerns the tangent space of the two kinds of fields. By the classical approach, the differential $d\boldsymbol{x}$ of a linear vector field is considered independently of the differential $d\boldsymbol{\alpha} = \boldsymbol{\varphi}_d\times\boldsymbol{\alpha}$ of an orthonormal field, which is controlled by the differential rotation vector $\boldsymbol{\varphi}_d$. By the proposed approach, instead, a unique differential $d\boldsymbol{A} = \boldsymbol{\eta}_d\times\boldsymbol{A}$ of an orthonormal dual field, controlled by the differential helix $\boldsymbol{\eta}_d$, is considered. On evaluation of the explicit form $\boldsymbol{\eta}_d = \boldsymbol{\varphi}_d + \epsilon\,\boldsymbol{\rho}_d$ of the differential helix, the angular part is seen to be just the differential rotation vector $\boldsymbol{\varphi}_d$, while the linear part is found to depend on both the characteristic differentials of the position and orientation fields, $\boldsymbol{\rho}_d = \boldsymbol{\Phi}\,d(\boldsymbol{\Phi}^{\mathrm{T}}\boldsymbol{x})$ $= d\boldsymbol{x} + \boldsymbol{x}\times\boldsymbol{\varphi}_d$. That means that the projection of the position out of a point is controlled by either parts of the dual differential helix, i.e. $d\boldsymbol{x} = \boldsymbol{\rho}_d - \boldsymbol{x}\times\boldsymbol{\varphi}_d$. In other words, the orientation field contributes to define the position itself of neighboring points, and the position and orientation become integrally coupled in a unique, dual field.

These considerations bring to establish a new modeling of the continuum relying on the pole-based oriento-position tensor field as configuration variable. It is referred

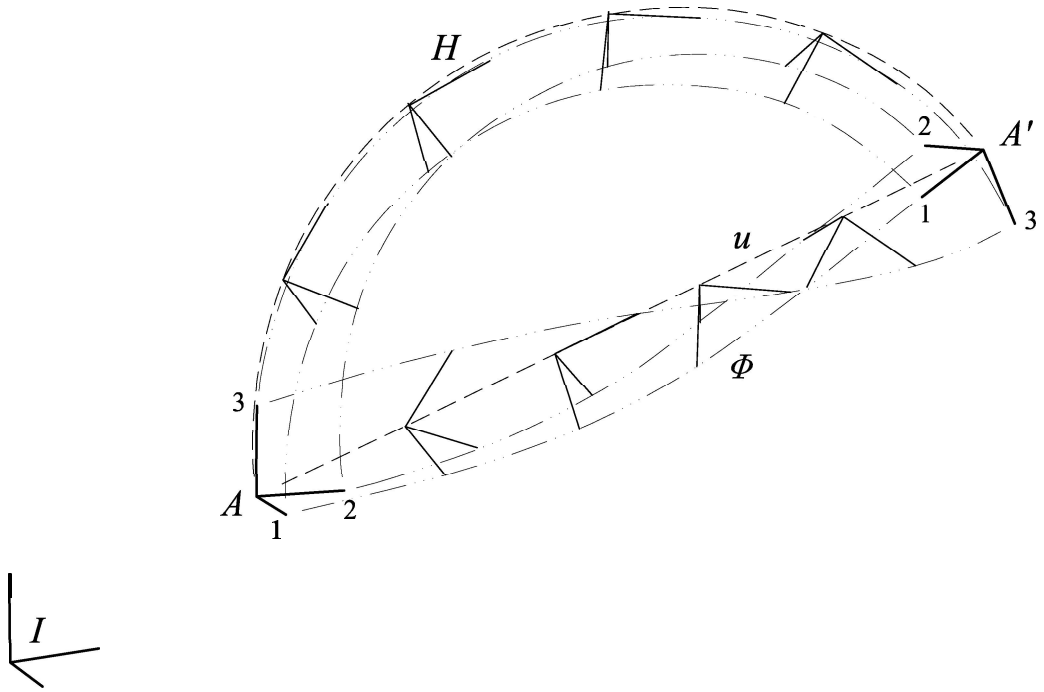

Figure 1: Helicoidal modeling ($\boldsymbol{H}$) against classical modeling ($\boldsymbol{u}$, $\boldsymbol{\Phi}$) in the motion of a frame

to as *helicoidal modeling* since a differential helix characterizes the tangent space of the configuration field. The outline of the proposed modeling against the classical one is traced in Figure 1, where the deep difference between the tangent spaces is noted (either are constant-curvature paths). The explicit dependence on a pole is inherent in this modeling; however, the choice of the pole is arbitrary, and it is just a matter of convenience to make it coincident with the origin of the absolute reference frame. Note that by self-basing the differential helix on the current point itself, the resulting dual vector $\boldsymbol{X}^{\mathrm{T}}\boldsymbol{\eta}_d = \boldsymbol{\varphi}_d + \epsilon\, d\boldsymbol{x}$ embodies just the separate characteristic differentials of the orientation and position fields, and the modeling of the continuum falls within the classical case.

In our opinion, the helicoidal way of modeling a continuum with oriented particles is much more natural than the classical way, and constitutes the best kinematical starting point for frame invariant approximations of variational formulations in solid mechanics. However, difficulties are encountered in this context when differentiating the field of orthonormal oriento-positions, since three independent variations must be considered synchronously: the spatial differentiation describing the curvature, the incremental differentiation relevant to the solution procedure and the virtual differentiation inherent in the variational setting. This entails mixed differentiations and leads to define as for Eqs. (2) mixed characteristic differentials.

4 Continuum description and variational setting

Let's denote with $\boldsymbol{A}'$ the oriento-position of a material particle in the current configuration, and take independent variations in either the virtual (δ), incremental (∂)

and spatial sense. On use of Eqs. (2), it is found that [12, 13]

$$\begin{aligned}
\boldsymbol{A}'^{\mathrm{T}}\boldsymbol{A}'_{/\otimes} &= (\boldsymbol{A}'^{\mathrm{T}}\boldsymbol{k}')^{\times} \\
\boldsymbol{A}'^{\mathrm{T}}\delta\boldsymbol{A}' &= (\boldsymbol{A}'^{\mathrm{T}}\boldsymbol{a}'_{\delta})\times \\
\boldsymbol{A}'^{\mathrm{T}}\partial\boldsymbol{A}' &= (\boldsymbol{A}'^{\mathrm{T}}\boldsymbol{a}'_{\partial})\times \\
\boldsymbol{A}'^{\mathrm{T}}\partial\delta\boldsymbol{A}' &= (\boldsymbol{A}'^{\mathrm{T}}\boldsymbol{a}'_{\partial\delta})\times + \tfrac{1}{2}\left((\boldsymbol{A}'^{\mathrm{T}}\boldsymbol{a}'_{\delta})\times(\boldsymbol{A}'^{\mathrm{T}}\boldsymbol{a}'_{\partial})\times + (\boldsymbol{A}'^{\mathrm{T}}\boldsymbol{a}'_{\partial})\times(\boldsymbol{A}'^{\mathrm{T}}\boldsymbol{a}'_{\delta})\times\right) \\
\boldsymbol{A}'^{\mathrm{T}}\delta\boldsymbol{A}'_{/\otimes} &= (\boldsymbol{A}'^{\mathrm{T}}\boldsymbol{k}'_{\delta})^{\times} - \tfrac{1}{2}(\boldsymbol{A}'^{\mathrm{T}}\boldsymbol{a}'_{\delta}\times\boldsymbol{k}')^{\times} + (\boldsymbol{A}'^{\mathrm{T}}\boldsymbol{a}'_{\delta})\times(\boldsymbol{A}'^{\mathrm{T}}\boldsymbol{k}')^{\times} \\
\boldsymbol{A}'^{\mathrm{T}}\partial\boldsymbol{A}'_{/\otimes} &= (\boldsymbol{A}'^{\mathrm{T}}\boldsymbol{k}'_{\partial})^{\times} - \tfrac{1}{2}(\boldsymbol{A}'^{\mathrm{T}}\boldsymbol{a}'_{\partial}\times\boldsymbol{k}')^{\times} + (\boldsymbol{A}'^{\mathrm{T}}\boldsymbol{a}'_{\partial})\times(\boldsymbol{A}'^{\mathrm{T}}\boldsymbol{k}')^{\times} \\
\boldsymbol{A}'^{\mathrm{T}}\partial\delta\boldsymbol{A}'_{/\otimes} &= (\boldsymbol{A}'^{\mathrm{T}}\boldsymbol{k}'_{\partial\delta})^{\times} - \tfrac{1}{2}(\boldsymbol{A}'^{\mathrm{T}}\boldsymbol{a}'_{\partial\delta}\times\boldsymbol{k}')^{\times} + (\boldsymbol{A}'^{\mathrm{T}}\boldsymbol{a}'_{\partial\delta})\times(\boldsymbol{A}'^{\mathrm{T}}\boldsymbol{k}')^{\times} \\
&\quad -\tfrac{1}{2}(\boldsymbol{A}'^{\mathrm{T}}\boldsymbol{a}'_{\delta}\times\boldsymbol{k}'_{\partial} + \boldsymbol{A}'^{\mathrm{T}}\boldsymbol{a}'_{\partial}\times\boldsymbol{k}'_{\delta})^{\times} \\
&\quad +(\boldsymbol{A}'^{\mathrm{T}}\boldsymbol{a}'_{\delta})\times(\boldsymbol{A}'^{\mathrm{T}}\boldsymbol{k}'_{\partial})^{\times} + (\boldsymbol{A}'^{\mathrm{T}}\boldsymbol{a}'_{\partial})\times(\boldsymbol{A}'^{\mathrm{T}}\boldsymbol{k}'_{\delta})^{\times},
\end{aligned} \tag{3}$$

where $(\,)_{/\otimes}$ is a notation for the gradient $(\,)_{,i}\otimes\boldsymbol{g}^i$, and the 'tensor-cross' notation $(\,)^{\times} = (\,)_i\times\otimes\boldsymbol{g}^i$ denotes a 3rd-order tensor with skew-symmetric tensor components (as for a Lagrangian approach, $\boldsymbol{g}_i$ and $\boldsymbol{g}^i$ are the covariant and contravariant base vectors of the reference configuration). Eqs. (3) define 7 characteristic differential dual tensors: the current (finite) curvature $\boldsymbol{k}'$, the virtual, incremental and mixed virtual-incremental oriento-position vectors $\boldsymbol{a}'_{\delta}$, $\boldsymbol{a}'_{\partial}$, $\boldsymbol{a}'_{\partial\delta}$, and the virtual, incremental and mixed virtual-incremental curvatures $\boldsymbol{k}'_{\delta}$, $\boldsymbol{k}'_{\partial}$, $\boldsymbol{k}'_{\partial\delta}$.

In order to define a strain measure, let's introduce the rototranslation field from the reference configuration to the current one, by putting $\boldsymbol{A}' = \boldsymbol{H}\boldsymbol{A}$. Again, a dual tensor $\boldsymbol{\omega}$ characterizes the gradient of the rototranslation field, $\boldsymbol{H}^{\mathrm{T}}\boldsymbol{H}_{/\otimes} = (\boldsymbol{H}^{\mathrm{T}}\boldsymbol{\omega})^{\times}$; moreover, that tensor is seen to represent the following change of curvature,

$$\boldsymbol{\omega} = \boldsymbol{k}' - \boldsymbol{H}\boldsymbol{k}, \tag{4}$$

where $\boldsymbol{k}$ is the reference curvature such that $\boldsymbol{A}^{\mathrm{T}}\boldsymbol{A}_{/\otimes} = (\boldsymbol{A}^{\mathrm{T}}\boldsymbol{k})^{\times}$. Now, a rigid motion is characterized by a unique rototranslation $\boldsymbol{H}$ [13], and in this case the curvature undergoes a rototranslation to $\boldsymbol{k}' = \boldsymbol{H}\boldsymbol{k}$ and tensor $\boldsymbol{\omega}$ is null. Therefore, $\boldsymbol{\omega}$ represents the appropriate kinematical measure of strain, and will be shortly referred to as *strain tensor*.

A polar material capable of couple-stressing is first considered. On use of dual tensors, the (static) balance of forces and moments with respect to the origin can be cast in the compact and meaningful form of equations [13]

$$\tilde{\boldsymbol{S}}_{/\bullet} + \boldsymbol{b} = \boldsymbol{0} \tag{5}$$

$$\tilde{\boldsymbol{S}}\boldsymbol{\nu} = \boldsymbol{s}\,, \tag{6}$$

applying respectively to the body volume (with $(\,)_{/\bullet}$ denoting the divergence $(\,)_{,i}\cdot\boldsymbol{g}^i$) and to the body surface (of outward normal $\boldsymbol{\nu}$). Here, $\tilde{\boldsymbol{S}} = \boldsymbol{X}'(\tilde{\boldsymbol{T}} + \epsilon\,\tilde{\boldsymbol{M}})$ is the pole-based dual stress tensor, with $\tilde{\boldsymbol{T}}$ the 1st Piola-Kirchhoff stress tensor, $\tilde{\boldsymbol{M}}$ the corresponding couple-stress tensor and $\boldsymbol{X}'$ the arm operator of the current point; $\boldsymbol{b} = \boldsymbol{X}'(\boldsymbol{f} + \epsilon\,\boldsymbol{c})$ and $\boldsymbol{s} = \boldsymbol{X}'(\boldsymbol{t} + \epsilon\,\boldsymbol{m})$ are the pole-based load densities per unit reference volume and surface, respectively, with $\boldsymbol{f}$ and $\boldsymbol{t}$ the acting forces and $\boldsymbol{c}$ and $\boldsymbol{m}$ the acting couples.

For a hyperelastic material with strain energy $w(\boldsymbol{\xi})$, the strain parameter $\boldsymbol{\xi}$ and the work-conjugate stress parameter

$$\hat{\boldsymbol{S}} = w_{/\boldsymbol{\xi}} \tag{7}$$

become identified as the self-based dual tensors

$$\boldsymbol{\xi} = \boldsymbol{X}^{\mathrm{T}}\boldsymbol{H}^{\mathrm{T}}\boldsymbol{\omega} = \boldsymbol{\Phi}^{\mathrm{T}}\boldsymbol{X}'^{\mathrm{T}}\boldsymbol{\omega} \tag{8}$$

$$\hat{\boldsymbol{S}} = \boldsymbol{X}^{\mathrm{T}}\boldsymbol{H}^{\mathrm{T}}\tilde{\boldsymbol{S}} = \boldsymbol{\Phi}^{\mathrm{T}}\boldsymbol{X}'^{\mathrm{T}}\tilde{\boldsymbol{S}}\,, \tag{9}$$

i.e. the pole-based strain and stress tensors $\boldsymbol{\omega}$ and $\tilde{\boldsymbol{S}}$, back-rototranslated and then self-based (or equivalently, self-based and then back-rotated).

Eqs. (5), (7) and (8) represent the equilibrium, constitutive and compatibility equations of a three-field elastic problem in continuum mechanics, with the configuration $\boldsymbol{A}'$ and the strain and stress parameters $\boldsymbol{\xi}$ and $\hat{\boldsymbol{S}}$ as unknowns. The balance Eq. (6) and the compatibility statement

$$\log \boldsymbol{H} = \log \boldsymbol{H}_b\,, \tag{10}$$

which enforces the logarithm of the rototranslation to comply with a boundary value, are the boundary conditions of the problem. From the calculus of variations, the weak form of the problem follows. On use of physical, consistent virtual multipliers, a general variational principle is drawn [13],

$$\begin{aligned}\int_V \Big\{\delta\Big[w - \langle\hat{\boldsymbol{S}}, (\boldsymbol{\xi} - \boldsymbol{X}^{\mathrm{T}}\boldsymbol{H}^{\mathrm{T}}\boldsymbol{\omega})\rangle\Big] - \langle\boldsymbol{a}'_\delta, \boldsymbol{b}\rangle\Big\}\,dV \\ - \int_S \Big\{\langle\boldsymbol{a}'_\delta, \boldsymbol{s}\rangle + \langle\delta(\boldsymbol{\Lambda}\boldsymbol{X}\hat{\boldsymbol{S}}\boldsymbol{\nu}), \mathrm{ax}(\log\boldsymbol{H} - \log\boldsymbol{H}_b)\rangle\Big\}\,dS = 0\,,\end{aligned}$$

which corresponds to the well-known Principle of Hu-Washizu. (The scalar product between dual tensors of the kinematical and co-kinematical spaces is resolved in such a way that, e.g., $\langle\boldsymbol{a}'_\delta, \boldsymbol{b}\rangle = \langle\mathrm{primal}(\boldsymbol{a}'_\delta), \mathrm{dual}(\boldsymbol{b})\rangle + \langle\mathrm{dual}(\boldsymbol{a}'_\delta), \mathrm{primal}(\boldsymbol{b})\rangle$.)

The foregoing variational setting is suitable for the non-polar continuum as well, once appropriate restrictions are assumed as regards the dependency relations of the strain energy. Following [11], a so-called pseudo-polar continuum is first introduced by postulating the strain energy to be independent of the angular part of the strain parameter, so discarding the couple-stress. The strain and stress parameters reduce to the linear parts and become identified by real tensors $\boldsymbol{\varepsilon} = \mathrm{dual}(\boldsymbol{X}^{\mathrm{T}}\boldsymbol{H}^{\mathrm{T}}\boldsymbol{\omega})$ and $\hat{\boldsymbol{T}} = \boldsymbol{\Phi}^{\mathrm{T}}\tilde{\boldsymbol{T}}$ (the Biot-Lur'e stress tensor). Then, a second constitutive postulate leads to the non-polar continuum: with reference to the Euclidean decomposition $\hat{\boldsymbol{T}} = \hat{\boldsymbol{T}}^{\mathrm{S}} + \hat{\boldsymbol{\tau}}\times$ of the stress parameter, the complementary energy $v(\hat{\boldsymbol{T}})$ is assumed to be independent of the skew-symmetric part $\hat{\boldsymbol{\tau}}\times$. This yields a hyperelastic framework based on symmetrical strain and stress work-conjugate parameters, namely $\boldsymbol{\varepsilon}^{\mathrm{S}}$ and $\hat{\boldsymbol{T}}^{\mathrm{S}} = w_{/\boldsymbol{\varepsilon}^{\mathrm{S}}}$. However, the axial $\hat{\boldsymbol{\tau}}$ of the Biot stress remains as a workless field and becomes a primary unknown. Conformingly, part of the compatibility condition reduces to the mere kinematical constraint $\mathrm{dual}\,\mathrm{ax}(\boldsymbol{X}^{\mathrm{T}}\boldsymbol{H}^{\mathrm{T}}\boldsymbol{\omega}) = 0$, which forces the polar decomposition theorem of the deformation gradient and becomes a governing equation of the problem.

For a non-polar continuum, by further assuming as fulfilled the constitutive and compatibility equations, the Principle of Virtual Work is drawn and takes the following 'constrained' form,

$$\int_V \left\{\delta\left[w + \langle\hat{\boldsymbol{\tau}}\times, \mathrm{dual}(\boldsymbol{X}^{\mathrm{T}}\boldsymbol{H}^{\mathrm{T}}\boldsymbol{\omega})\rangle\right] - \langle\boldsymbol{a}'_\delta, \boldsymbol{b}\rangle\right\} dV - \int_S \langle\boldsymbol{a}'_\delta, \boldsymbol{s}\rangle\, dS = 0\,, \tag{11}$$

with the oriento-position $\boldsymbol{A}'$ and the Biot-axial $\hat{\boldsymbol{\tau}}$ as the only unknowns. By linearizing Eq. (11) under the simplifying hypothesis of constant self-based loads $\boldsymbol{X}'^{\mathrm{T}}\boldsymbol{b}$ and $\boldsymbol{X}'^{\mathrm{T}}\boldsymbol{s}$, the incremental equation $\Pi_\delta + \partial\Pi_\delta = 0$ is obtained, with

$$\begin{aligned} \Pi_\delta \;=& \int_V \Big\{\langle\boldsymbol{A}'\delta(\boldsymbol{A}'^{\mathrm{T}}\boldsymbol{k}'), \tilde{\boldsymbol{S}}\rangle + \langle\delta\hat{\boldsymbol{\tau}}\times, \boldsymbol{\Phi}^{\mathrm{T}}\mathrm{dual}(\boldsymbol{X}'^{\mathrm{T}}\boldsymbol{\omega})\rangle \\ &\qquad -\langle\boldsymbol{X}'^{\mathrm{T}}\boldsymbol{a}'_\delta, \boldsymbol{X}'^{\mathrm{T}}\boldsymbol{b}\rangle\Big\}\, dV - \int_S \langle\boldsymbol{X}'^{\mathrm{T}}\boldsymbol{a}'_\delta, \boldsymbol{X}'^{\mathrm{T}}\boldsymbol{s}\rangle\, dS \end{aligned} \tag{12}$$

as virtual functional and $\partial\Pi_\delta = \partial\Pi_{\delta\mathrm{E}} + \partial\Pi_{\delta\mathrm{K}} + \partial\Pi_{\delta\mathrm{G}}$ as incremental variation, split into the elastic, the kinematical-constraint and the geometric contributions

$$\begin{aligned} \partial\Pi_{\delta\mathrm{E}} \;=& \int_V \boldsymbol{\Phi}^{\mathrm{T}}\mathrm{dual}(\boldsymbol{X}'^{\mathrm{T}}\boldsymbol{A}'\delta(\boldsymbol{A}'^{\mathrm{T}}\boldsymbol{k}')) : \mathbb{E} : \boldsymbol{\Phi}^{\mathrm{T}}\mathrm{dual}(\boldsymbol{X}'^{\mathrm{T}}\boldsymbol{A}'\partial(\boldsymbol{A}'^{\mathrm{T}}\boldsymbol{k}'))\, dV \\ \partial\Pi_{\delta\mathrm{K}} \;=& \int_V \Big\{\langle\delta\hat{\boldsymbol{\tau}}\times, \boldsymbol{\Phi}^{\mathrm{T}}\mathrm{dual}(\boldsymbol{X}'^{\mathrm{T}}\boldsymbol{A}'\partial(\boldsymbol{A}'^{\mathrm{T}}\boldsymbol{k}'))\rangle \\ &\qquad +\langle\partial\hat{\boldsymbol{\tau}}\times, \boldsymbol{\Phi}^{\mathrm{T}}\mathrm{dual}(\boldsymbol{X}'^{\mathrm{T}}\boldsymbol{A}'\delta(\boldsymbol{A}'^{\mathrm{T}}\boldsymbol{k}'))\rangle \\ &\qquad +\langle\partial\delta\hat{\boldsymbol{\tau}}\times, \boldsymbol{\Phi}^{\mathrm{T}}\mathrm{dual}(\boldsymbol{X}'^{\mathrm{T}}\boldsymbol{\omega})\rangle\Big\}\, dV \\ \partial\Pi_{\delta\mathrm{G}} \;=& \int_V \Big\{\langle\boldsymbol{A}'\partial\delta(\boldsymbol{A}'^{\mathrm{T}}\boldsymbol{k}'), \tilde{\boldsymbol{S}}\rangle - \langle\partial(\boldsymbol{X}'^{\mathrm{T}}\boldsymbol{a}'_\delta), \boldsymbol{X}'^{\mathrm{T}}\boldsymbol{b}\rangle\Big\}\, dV \\ &\qquad - \int_S \langle\partial(\boldsymbol{X}'^{\mathrm{T}}\boldsymbol{a}'_\delta), \boldsymbol{X}'^{\mathrm{T}}\boldsymbol{s}\rangle\, dS\,. \end{aligned} \tag{13}$$

In Eqs. (12) and (13), $\tilde{\boldsymbol{S}}$ is computed as $\boldsymbol{H}\boldsymbol{X}(w_{/\boldsymbol{\varepsilon}^{\mathrm{S}}} + \hat{\boldsymbol{\tau}}\times)$ and $\mathbb{E} = w_{/\boldsymbol{\varepsilon}^{\mathrm{S}}\boldsymbol{\varepsilon}^{\mathrm{S}}}$ is the 4^{th}-order elastic tensor. The linearized principle also depends on the virtual, incremental and mixed virtual-incremental variation variables $\boldsymbol{a}'_\delta$, $\boldsymbol{a}'_\partial$, $\boldsymbol{a}'_{\partial\delta}$, $\boldsymbol{k}'_\delta$, $\boldsymbol{k}'_\partial$, $\boldsymbol{k}'_{\partial\delta}$, defined in Eqs. (3), and on $\delta\hat{\boldsymbol{\tau}}$, $\partial\hat{\boldsymbol{\tau}}$, $\partial\delta\hat{\boldsymbol{\tau}}$. The mixed variation variables are in general not null in a finite-element approximation, unless the field variables are assumed to depend linearly on the discrete set of nodal variables.

5 Discrete helicoidal modeling

A consistent approximation of the variational problem Eq. (11) relies on a substitute model of the continuum and of the evolution of its configuration, respectful of the underlying helicoidal modeling. So, a suitable finite element requires a *multiplicative interpolation* scheme of the oriento-position, i.e. based on the rototranslations from the nodal oriento-positions [15]. The interpolated oriento-position $\boldsymbol{A}'$ among given nodal values $\boldsymbol{A}'_J$ $(J = 1, 2, ...N)$ is obtained by weighting appropriate 'distances', which are represented, in a space of orthogonal transformations, by the logarithms of the relative rototranslations $\boldsymbol{A}'\boldsymbol{A}'^{\mathrm{T}}_J$, namely the relative *helices*. The weighted average oriento-position is sought with an implicit interpolation formula,

$$\sum_{J=1,...N} W_J \log(\boldsymbol{A}'\boldsymbol{A}'^{\mathrm{T}}_J) = \boldsymbol{0}\,, \tag{14}$$

which is numerically solved by a Newton-Raphson procedure. Note that this is in contrast with weighting the helices defining the nodal oriento-positions themselves, and yields a frame-invariant interpolation scheme, able to reproduce exactly any rigid body motion [4].

Linearization of the interpolation formula Eq. (14) in the threefold sense (spatial, virtual and incremental) yields the finite curvature $\boldsymbol{k}'$ and explicit expressions for the operators linearly relating the local variation variables $\boldsymbol{a}'_{\delta}$, $\boldsymbol{a}'_{\partial}$, $\boldsymbol{a}'_{\partial\delta}$, $\boldsymbol{k}'_{\delta}$, $\boldsymbol{k}'_{\partial}$, $\boldsymbol{k}'_{\partial\delta}$ to the virtual, incremental and mixed virtual-incremental nodal oriento-position dual vectors $\boldsymbol{a}'_{\delta J}$, $\boldsymbol{a}'_{\partial J}$, $\boldsymbol{a}'_{\partial\delta J}$, see [14, 15]. The other kinematical variation variables appearing in Eqs. (12)-(13) are worked out with the help of Eqs. (3)-(4) [13].

As far as concerns the substitute field of the Biot-axial variable, it is worth pointing out the role of the workless stress $\hat{\boldsymbol{\tau}}$ in Eq. (11): that of bringing the kinematical rotation to coincide with the rotation defined through the polar decomposition of the deformation gradient. It is also worth noting that in the helicoidal modeling, positions and orientations are coupled in such a way that a nodal rotation induces a local variation of the deformation gradient, hence elastic strains and stresses. However, combinations of nodal rotations exist that do not affect the deformation gradient, and withstanding such intrinsic rotation modes is exactly the role of the substitute Biot-axial field. For a solid element with eight corner nodes, a *three-linear Biot-axial field* depending on the six scalar components $\hat{\tau}_I$ $(I = 1, 2, ...6)$ normal to each face proves successful. According to this interpolation scheme, the normal components of the Biot-axial are continuous. The linearization is straightforward, and in particular it results $\partial\delta\hat{\boldsymbol{\tau}} = \boldsymbol{0}$.

On use of such interpolations for the kinematical and Biot-axial fields within Eqs. (12) and (13), and of multilinear weight functions, an 8-nodes/6-faces volume element is formulated (48 kinematical unknowns plus 6 Biot-axial). To introduce the boundary loads, a 4-nodes surface element is also provided (24 kinematical unknowns). The corresponding planar elements for 2D computations are the 4-nodes/1-face volume element (12 kinematical unknowns plus a single Biot-axial component normal to the plane) and the 2-nodes surface element (6 kinematical unknowns).

The *helicoidal element* is still relating virtual, incremental and mixed virtual-incremental discrete variation variables, namely the differential helices $\boldsymbol{\eta}_{\delta J} \equiv \boldsymbol{a}'_{\delta J}$, $\boldsymbol{\eta}_{\partial J} \equiv \boldsymbol{a}'_{\partial J}$ and $\boldsymbol{\eta}_{\partial\delta J} \equiv \boldsymbol{a}'_{\partial\delta J}$ of the nodal rototranslations $\boldsymbol{H}_J = \boldsymbol{A}'_J \boldsymbol{A}_J^{\mathrm{T}}$, and the Biot-axial variations $\delta\hat{\tau}_I$ and $\partial\hat{\tau}_I$ at the faces. Before dropping the column of the virtual multipliers to obtain a set of equations in the incremental unknowns $\boldsymbol{\eta}_{\partial J}$ and $\partial\hat{\tau}_I$, the

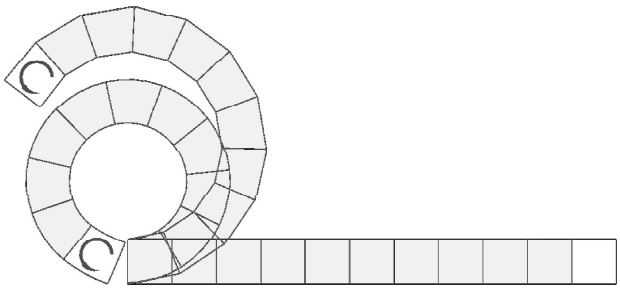

Figure 2: 2D beam roll-up. Comparison with classical modeling

mixed variation variables must be solved for the virtual and incremental variables separately. This is accomplished at the nodal level, where the mixed variations $\partial\delta$ of the primitive variables $\boldsymbol{\eta}_J$ are assumed null and the 2nd-order differential map of the rototranslation [14] enables writing $\boldsymbol{\eta}_{\partial\delta J} = \boldsymbol{\Lambda}_{\mathrm{III}\,J} : \boldsymbol{\Lambda}_J^{-1}\boldsymbol{\eta}_{\delta J} \otimes \boldsymbol{\Lambda}_J^{-1}\boldsymbol{\eta}_{\partial J}$, with $\boldsymbol{\Lambda}_J$ and $\boldsymbol{\Lambda}_{\mathrm{III}\,J}$ (a 3rd-order dual tensor symmetrical on the rightmost indexes) the first and second differential mapping tensors associated with $\boldsymbol{H}_J$.

It is inherent in the helicoidal modeling to update multiplicatively the kinematical variables during the iterative solution process. The updated nodal oriento-positions are obtained from the preceding ones by rototranslations built with the incremental helices, $\boldsymbol{A}_J'^{\,n+1} = \exp(\boldsymbol{\eta}_{\partial J}\times)\,\boldsymbol{A}_J'^{\,n}$. The Biot-axial variables are linearly updated, $\hat{\tau}_I^{n+1} = \hat{\tau}_I^n + \partial\hat{\tau}_I$.

6 Examples

Some examples are given of highly distorting solids in geometrically nonlinear loading histories. It is worth stressing that in the images, the rendered geometry as well is helicoidally interpolated from the corner oriento-positions.

The in-plane roll-up of a slender membrane clamped at one end and bent by a tip couple is analyzed as an elastic plane-stress problem ($E = 1200$, $\nu = 0.3$). A complete circle is achieved under a couple $M = \kappa\, 2\pi EJ/l$, with κ a correction factor accounting for low aspect ratio l/h ($\kappa = 0.9255$ for a 10×1 membrane) [11]. In spite of a very coarse mesh (ten square elements plus the tip carrying the volume couple), the high performance in bending of the 2D element is evidenced in Figure 2, as compared with the early result under classical modeling, based on constant rotation and Biot-axial over the element [11]. The analysis of this problem using 4-node elements with interpolated rotations proved even stiffer [7, 8], while a satisfactory result was only achieved by resorting to incompatible modes.

The 3D version of this example refers to a beam 1×1×10. Since no correction factor is available for this case, the same value $\kappa = 0.9255$ as for plane-stress is assumed. The initial and final configurations for 6 different models are shown in Figure 3. The helicoidal element exhibits an excellent capacity of modeling constant-curvature

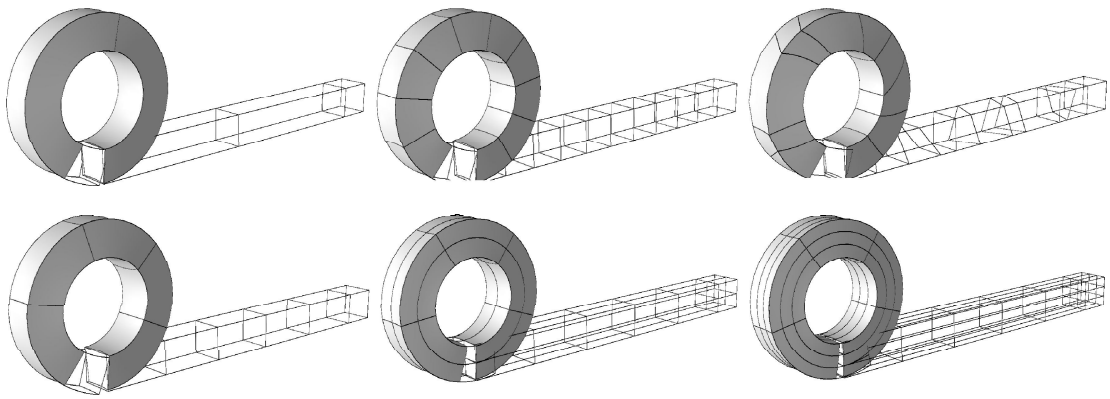

Figure 3: 3D beam roll-up with six different models

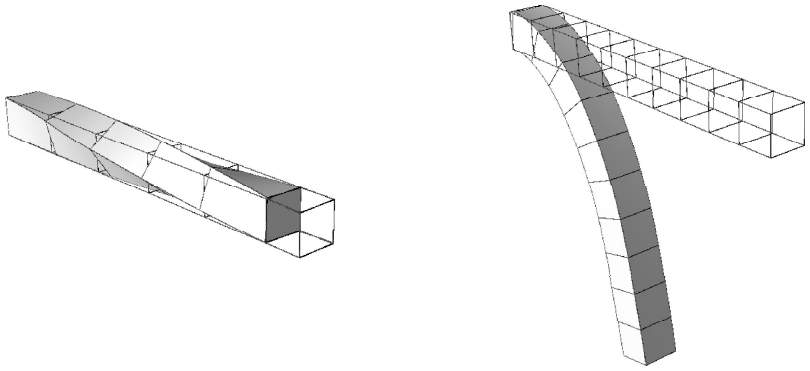

Figure 4: Beam twist and bending

geometries. In fact, the results are insensitive to the mesh refinement along the beam axis, and the deformation with 2, 5 or 10 elements (with a single element over the beam section) is in any case comparable with the 2D case. Also the insensitivity to irregular meshes is fairly good. The convergence of the element is proved by the closing of the circle as the mesh is refined on the cross-section.

The same beam is tested in torsion (by a twisting couple within the appended tip element) and in bending-shear (by a transverse force on the butt-surface). In torsion, the response is almost linear, and under a torque $M = \pi G J_{\mathrm{P}}/2l$ the tip rotation is very close to $\pi/2$. The deformation under a transverse tip force $F = 10$ is in agreement with results from literature [7, 8, 9] (the tip displacement is 5.39 horizontal and 8.15 vertical).

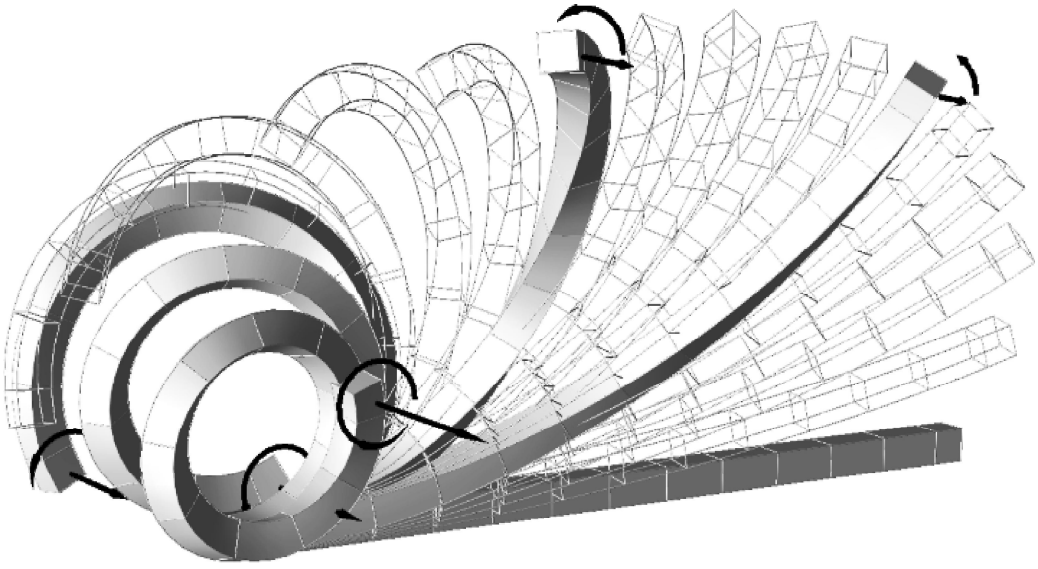

Figure 5: Wrenching beam

The example of a clamped beam wrenched by a tip force and a coaxial couple

evidences how the proposed modeling is fit for large 3D rotations. A beam $1\times1\times25$ in size, of elastic properties $E = 1200$ and $\nu = 0.3$, is modelled by 13 elements (the last, cubic element carries the load within the volume). The loads are made growing simultaneously up to the final force $F = 1.8$ and couple $M = 36$. In Figure 5, the large curling up to more than 450° is frozen every 20% of the load history. In this case of non-conservative loading, the response is characterized by a fast change of configuration between about 40% and 60%, in the course of which the force is observed to do a negative work. The same case, analyzed by a classical modeling relying on discontinuous rotation and Biot-axial, was much stiffer [11].

The solution of the nonlinear examples above is in general rather slow due to the small load steps required — apart from the nearly linear case of twist, when 6 iterations suffice to reach convergence for the full load in one step. For the 2D and 3D roll-up and bending-shear with one element across the beam section, increments of 5% are used and occasionally reduced to 2.5%. With two and three elements across the beam section, increments of 2.5% prove necessary since the 40% of the load history. The wrenched beam is solved with 2% load increments up to the 30%, and then with 1%-steps occasionally halved to 0.5%. Within each step, the convergence is always attainable with a quadratic rate and in most cases in 5-6 iterations.

7 Conclusion

It is quite evident that the power of the proposed helicoidal modeling emerges just in the discrete approximations. In particular, the strongest difference against classical modeling is observable in the substitute kinematical field over the element domain, consistent with the underlying helicoidal modeling. This method is then promising in computational finite elasticity, since it can improve in quality the geometrically nonlinear analysis of largely curving solids, as the given examples evidence.

References

[1] Angeles, J., 1998. The application of dual algebra to kinematic analysis. In: Angeles, J., Zakhariev, E. (Eds.), Computational Methods in Mechanical Systems. Springer-Verlag, Heidelberg, Vol. 161, pp 1-31.

[2] Atluri, S.N., Cazzani, A., 1995. Rotations in computational solid mechanics. Arch. Comput. Meth. Engng 2, 49-138.

[3] Borri, M., Trainelli, L., Bottasso, C.L., 2000. On representations and parameterizations of motion. Multibody System Dynamics 4, 129-193.

[4] Crisfield, M., Jelenic, G., 1999. Objectivity of strain measures in the geometrically exact three dimensional beam theory and its finite-element implementation. Proc. R. Soc. Lond. A 455, 1125-1147.

[5] Grekova, E., Zhilin, P., 2001. Basic equations of Kelvin's medium and analogy with ferromagnets. J. Elasticity 64, 29-70.

[6] Hughes, T.J.R., Brezzi, F., 1989. On drilling degrees of freedom. Comp. Meth. Appl. Mech. Engng 72, 105-121.

[7] Ibrahimbegović, A., Frey, F. 1993. Geometrically non-linear method of incompatible modes in application to finite elasticity with independent rotations. Int. J. Numer. Meth. Engng 36, 4185-4200.

[8] Ibrahimbegović, A., Frey, F. 1995. Variational principles and membrane finite elements with drilling rotations for geometrically nonlinear elasticity. Int. J. Numer. Meth. Engng 38, 1885-1900.

[9] Kožar, I. and Ibrahimbegović, A., 1995. Finite element formulation of the finite rotation solid element. Finite Elements Anal. Des. 20, 101-126.

[10] Le, K.C., Stumpf, H., 1998. Strain measures, integrability condition and frame indifference in the theory of oriented media. Int. J. Solids Struct. 35, 783-798.

[11] Merlini, T., 1997. A variational formulation for finite elasticity with independent rotation and Biot-axial fields. Computat. Mech. 19, 153-168.

[12] Merlini, T., 2002. Differentiation of rotation and rototranslation. DIA-SR 02-16, Dip. Ing. Aerospaziale, Politecnico di Milano.

[13] Merlini, T., Morandini, M., 2002. Variational formulations for helicoidal modeling in finite elasticity. DIA-SR 02-17, Dip. Ing. Aerospaziale, Politecnico di Milano.

[14] Merlini, T., 2003. Recursive representation of orthonormal tensors. DIA-SR 03-02, Dip. Ing. Aerospaziale, Politecnico di Milano.

[15] Merlini, T., Morandini, M., 2003. Interpolation of the orientation and orientoposition fields. DIA-SR 03-03, Dip. Ing. Aerospaziale, Politecnico di Milano.

[16] Merlini, T., Morandini, M., 2003. The helicoidal modeling in computational finite elasticity. (Submitted for publication.)

[17] Nikitin, E., Zubov, L.M., 1998. Conservation laws and conjugate solutions in the elasticity of simple materials and materials with couple stress. J. Elasticity 51, 1-22.

[18] Simo, J.C., Fox, D.D., Hughes, T.J.R., 1992. Formulation of finite elasticity with independent rotations. Comp. Meth. Appl. Mech. Engng 95, 277-288.

[19] Wisniewski, K., 1998. A shell theory with independent rotations for relaxed Biot stress and right stretch strain. Computat. Mech. 21, 101-122.

[20] Zubov, L.M., 1990. Variational principles and invariant integrals for nonlinearly elastic bodies with couple stress. Izvestiya Akademy Nauk SSSR Mehanika Tverdogo Tela 25, 10-16. Translation in: Mechanics of Solids 25, 7-13.

Teodoro Merlini, Marco Morandini, Dipartimento di Ingegneria Aerospaziale, Politecnico di Milano, Italy